Neutron scattering evidence for fast ionic oxygen diffusion in the high temperature phases of La2O3

P. Aldebert, A.J. Dianoux, J.P. Traverse

▶ **To cite this version:**

P. Aldebert, A.J. Dianoux, J.P. Traverse. Neutron scattering evidence for fast ionic oxygen diffusion in the high temperature phases of La2O3. Journal de Physique, 1979, 40 (10), pp.1005-1012. 10.1051/jphys:0197900400100100500 . jpa-00209177

HAL Id: jpa-00209177
https://hal.science/jpa-00209177

Submitted on 4 Feb 2008

HAL is a multi-disciplinary open access archive for the deposit and dissemination of scientific research documents, whether they are published or not. The documents may come from teaching and research institutions in France or abroad, or from public or private research centers.

L'archive ouverte pluridisciplinaire **HAL**, est destinée au dépôt et à la diffusion de documents scientifiques de niveau recherche, publiés ou non, émanant des établissements d'enseignement et de recherche français ou étrangers, des laboratoires publics ou privés.

Classification
Physics Abstracts
66.30H — 61.12

Neutron scattering evidence for fast ionic oxygen diffusion in the high temperature phases of La_2O_3

P. Aldebert, A. J. Dianoux

Institut Laue-Langevin, 156X, 38042 Grenoble, France

and J. P. Traverse

Equipe de Recherche sur l'Energie, Université Paul-Sabatier, 31077 Toulouse, France

(*Reçu le 6 avril 1979, révisé le 18 juin 1979, accepté le 18 juin 1979*)

Résumé. — La diffusion rapide de l'oxygène dans les phases de haute température H et X de La_2O_3 est mise en évidence à partir de l'analyse du bruit de fond de diffraction neutronique et des données de diffusion quasi-élastique des neutrons. Dans la phase X à 2 160 °C le coefficient d'autodiffusion translationnelle est de l'ordre de 3×10^{-5} cm^2/s et le temps moyen entre sauts sur des sites tétraédriques voisins est d'environ $1{,}4 \times 10^{-12}$ s. Ces valeurs sont de l'ordre de celles présentées par les bons conducteurs de type superionique.

Abstract. — Evidence for fast oxygen diffusion in the H and X high temperature phases of La_2O_3 is presented from neutron diffraction background analysis and neutron quasielastic scattering data. In the X phase at 2 160 °C the translational self diffusion coefficient is of the order of 3×10^{-5} cm^2/s and the mean time between jumps on neighbouring tetrahedral sites is around 1.4×10^{-12} s. These are typical values for good superionic conductors.

1. **Introduction.** — High temperature X-ray diffraction and solar furnace thermal analysis studies have already given evidence of the existence near the melting point of new crystalline phases for the first members of the rare-earth sesquioxide family [1]. At room temperature La_2O_3 and Nd_2O_3 exist under a trigonal form ($P\bar{3}m1$) wrongly called the A hexagonal form and transform into the H form ($P6_3/mmc$), which is really hexagonal, at about 2 000 °C and into the X cubic form at 2 100-2 150 °C. The melting point for La_2O_3 and Nd_2O_3 is about 2 300 °C.

Our recent neutron diffraction work [2] performed on the D1B multidetector at the ILL had led us to a crystallographic description of these high temperature forms in which there is considerable oxygen disorder. We have also proposed a crystallochemical model which describes satisfactorily the polymorphic forms of these sesquioxides. This model presents a high degree of oxygen disorder in the H and X phases which can be of static or dynamical origin.

In this paper we present new results obtained by inelastic neutron scattering, which show that the oxygen disorder is indeed of dynamical nature. Section 2 deals with a new interpretation of the diffuse scattering observed in the diffraction patterns of the high temperature phases of La_2O_3. This enables us to extract the normalized structure factor of diffusing oxygen atoms. In section 3 we present the first inelastic neutron scattering data obtained above 2 000 °C. The two high temperature phases H and X of La_2O_3 are characterized by a broad quasielastic contribution, which is direct evidence for fast diffusive motions. With the use of a simplified dynamical model for the X phase, and the knowledge of the oxygen structure factor obtained in section 2, we are able to give approximate values for the dynamical parameters describing the oxygen motions. The translational self diffusion coefficient is of the order of 3×10^{-5} cm^2/s and the residence time on the crystallographic tetrahedral sites is around 1.4×10^{-12} s for the X phase at 2 160 °C. These are typical values for superionic conductors.

2. **Diffraction background analysis.** — We have reconsidered the diffuse scattering intensity between the Bragg peaks of our La_2O_3 diffraction data performed at $\lambda = 2.4$ Å [2]. In order to improve the poor statistics, especially for the high temperature experiments, each point is the sum over five cells of the multidetector (Fig. 1). The intensity of the back-

Article published online by EDP Sciences and available at http://dx.doi.org/10.1051/jphys:0197900400100100500

ground I may be written as the sum of three components [3, 4].

$$I = I_{inc} + I_{TDS} + I_{EDS}$$

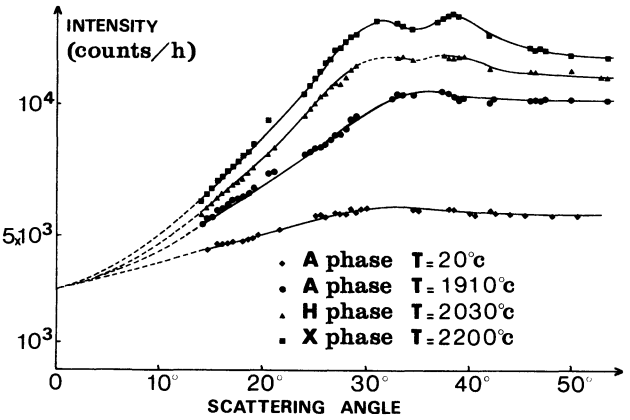

Fig. 1. — Evolution with temperature of the neutron diffraction background (λ = 2.4 Å) for La_2O_3. The missing points correspond to the Bragg peaks which are excluded in this analysis. The dashed-line at small scattering angles is an extrapolation of the measured background.

where :

— I_{inc} is the incoherent scattering intensity which is isotropic. It gives a constant contribution to the background which can be extracted from a reasonable extrapolation of the background to scattering angle $\theta = 0$;

— I_{TDS} is the thermal diffuse inelastic scattering (TDS) intensity which can be calculated in a first approximation for a given θ or Q (the momentum transfer $Q = \frac{4\pi \sin\theta}{\lambda}$) by the following formula :

$$I_{TDS} = \sum_{i=1}^{i=n} \{ 1 - \exp(-2W_i) \} b_i^2$$

with b_i the coherent scattering length of the atom i and

$$W_i = \frac{B_i^{th} \sin^2\theta}{\lambda^2}$$ the Debye-Waller factor

— I_{EDS} is the elastic diffuse scattering which originates from a local static structural disorder. As for the TDS, it corresponds to a loss of intensity in the Bragg peaks which can be estimated, to a first approximation, by a similar formalism in which appears as a pseudo Debye-Waller factor :

$$I_{EDS} = \sum_{i=1}^{i=n} \left\{1 - \exp\left(\frac{-2B_i^{dis}\sin^2\theta}{\lambda^2}\right)\right\} b_i^2.$$

The B factor obtained from structural refinements of the Bragg peak intensities is the sum of these two contributions $B = B^{th} + B^{dis}$.

In the case of diffusive motions of atoms another contribution, proportional to the structure factor $S(Q)$, is included in this term I_{EDS}.

On the basis of our crystallochemical model [2], we can assume for the A form at 1 910 °C that $I_{EDS} = 0$ because there is no static disorder and no diffusive motions giving rise to a quasielastic intensity. The background $I^A(\theta)$ can be expressed as follows

$$I^A(\theta) = I_{inc} + kI^A_{TDS}(\theta) \quad (1)$$

with k a proportionality constant related to the number of scattering centres and to the instrumental resolution. For La_2O_3 one has :

$$I^A_{TDS}(\theta) = 2\left\{1 - \exp\left(\frac{-2B^A_{La}\sin^2\theta}{\lambda^2}\right)\right\} b^2_{La} + 2\left\{1 - \exp\left(\frac{-2B^A_{Ox1}\sin^2\theta}{\lambda^2}\right)\right\} b^2_{Ox} + \left\{1 - \exp\left(\frac{-2B^A_{Ox2}\sin^2\theta}{\lambda^2}\right)\right\} b^2_{Ox}.$$

In the H phase at 2 030 °C we can postulate diffusive motions for the oxygen Ox2 founded on its high thermal B factor and the large La-Ox2 bond distance in the A phase at 1 910 °C [2]. The broadening of the Bragg peaks suggests also the existence of stresses inducing an oxygen static disorder in the (LaOx1) sheets. If we assume that the small increase of the B factor for lanthanum, between 1 910 °C and 2 030 °C (table 1) has a purely thermal origin, the same relative increase applied to the oxygen Ox1 would give a thermal B factor of 8.4 Å² instead of the refined value

Table I. — *Thermal B factor of the* La_2O_3 *phases at various temperatures refined from diffraction data*

		A phase room temperature	A phase T = 1 910 °C	H phase T = 2 030 °C, T = 2 060 °C (*)	$\frac{B_H - B_A}{B_A}$	X phase T = 2 160 °C and 2 230 °C (*)
La	B(Å²)	0.50 (2)	4.5 (5), 3.9 (2) (*)	5.4 (6), 5.8 (8) (*)	0.2, 0.46 (*)	8.8 (1.4) (*)
Ox1	B(Å²)	0.62 (4)	7.0 (1.2)	15.8 (1.7)	1.26	
Ox2	B(Å²)	0.82 (5)	14.9 (1.2)	17.9 (2.5)	0.2	

(*) Results from quasielastic experiments. In parenthesis is indicated the uncertainty on the last digit of the quoted value.

of 15.8 Å^2. The difference can be attributed to a static disorder. So we obtain :

$$I^{H}(\theta) = I_{inc} + kI^{H}_{TDS}(\theta) + I^{H}_{EDS(Ox1)} + I^{H}_{EDS(Ox2)} \quad (2)$$

with

$$I^{H}_{TDS}(\theta) = 2\left\{1 - \exp\left(\frac{-2B^{H}_{La}\sin^2\theta}{\lambda^2}\right)\right\} b^2_{La} + 2\left\{1 - \exp\left(\frac{-2B^{H}_{Ox1}\sin^2\theta}{\lambda^2}\right)\right\} b^2_{Ox}.$$

There is no contribution to $I^{H}_{TDS}(\theta)$ from the oxygen Ox2 due to its diffusive motion.

From (1) and (2) we can deduce the elastic and quasi-elastic diffuse intensity in the H form originating from the oxygen disorder

$$I^{H}_{EDS}(\theta) = I^{H}_{EDS(Ox1)} + I^{H}_{EDS(Ox2)} = I^{H}(\theta) - I_{inc} - \frac{(I^{A}(\theta) - I_{inc})\, I^{H}_{TDS}(\theta)}{I^{A}_{TDS}(\theta)} \quad (3)$$

In the X phase at 2 200 °C, the analysis of the Bragg peak intensities shows that the contribution of oxygens which are then all equivalent, is negligible [2]. This is evidence for a large oxygen disorder that we assume is originating from diffusive motions. The width of the Bragg peaks, reproducing the instrumental width, indicates no measurable static disorder in the lanthanum sublattice. The lanthanum thermal B factor used in this case comes from the quasielastic experiments because of the impossibility of obtaining a significant B factor from diffraction data [2]. So we obtain

$$I^{X}(\theta) = I_{inc} + kI^{X}_{TDS}(\theta) + I^{X}_{EDS(Ox)} \quad (4)$$

with

$$I^{X}_{TDS}(\theta) = 2\left\{1 - \exp\left(\frac{-2B^{X}_{La}\sin^2\theta}{\lambda^2}\right)\right\} b^2_{La}.$$

From (1) and (4) we find

$$I^{X}_{EDS}(\theta) = I^{X}(\theta) - I_{inc} - \frac{(I^{A}(\theta) - I_{inc})\, I^{X}_{TDS}(\theta)}{I^{A}_{TDS}(\theta)}. \quad (5)$$

The plots *versus* Q of (3) and (5) (not shown) exhibit the typical shape of a liquid like behaviour for the oxygens. The effects of absorption and multiple scattering can be readily neglected in comparison with the inelasticity effects due to the recoil of mobile oxygens caused by neutrons, which are taken into account by the Placzek correction. This can be expressed as [5] :

$$I_{obs}(Q) = NF\left\{\left(\frac{d\sigma}{d\Omega}\right)^{self}(1 + P(Q)) + \left(\frac{d\sigma}{d\Omega}\right)^{dis}_{coh}\right\}. \quad (6)$$

In a first approximation we can apply the same correction term $P(Q)$ to the distinct term which then becomes

$$I_{EDS(corrected)} = \frac{I_{EDS(observed)}}{1 + P(Q)}.$$

The correction term at the first order is expressed as

$$P(Q) = \frac{m_0}{2\overline{M}}\frac{k_B T}{E_0} - \left(C_1 + C_3\frac{k_B T}{E_0}\right)\frac{m_0}{\overline{M}}\left(\frac{Q}{k_0}\right)^2 \quad (7)$$

where m_0 is the mass, E_0 the energy and k_0 the wave-vector of the incident neutron ; $\overline{M}$ is the atomic mass of oxygen, k_B the Boltzmann constant, T the absolute temperature, C_1 and C_3 constants related to the efficiency of the detectors. At high values of Q (> 3.2 Å^{-1}), $P(Q)$ becomes negative and leads to overcorrections which show the limitations of the first order Placzek correction especially in the case of high values for the $k_B T/E_0$ ratio.

Nevertheless the plots of I_{EDS}(corr) and I_{EDS}(obs) allow a determination within some uncertainty for the I_{EDS} limit when $Q \to \infty$. This makes it possible to obtain the corresponding oxygen structure factor

$$S^{Ox}(Q) = \frac{I_{EDS(Q)}}{I_{EDS(\infty)}}$$

for the H and X phases. The errors bars for $S(Q)$ are estimated from uncertainties in the $I_{EDS}(\infty)$ determination (Figs. 2 and 3).

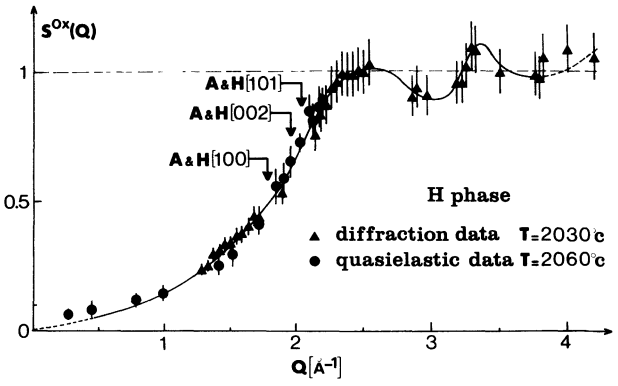

Fig. 2. — Q dependence of the normalized oxygen structure factor from diffraction background analysis and from quasielastic measurements for the H phase of La_2O_3. Positions of Bragg peaks in the A and H phases at high temperature are indicated in the overlapping Q range of the two techniques.

In the case of an assembly of identical particles the Debye formula [6] exhibits a first marked maximum for

$$Q_m = \frac{2\pi \times 1.23}{x_m}$$

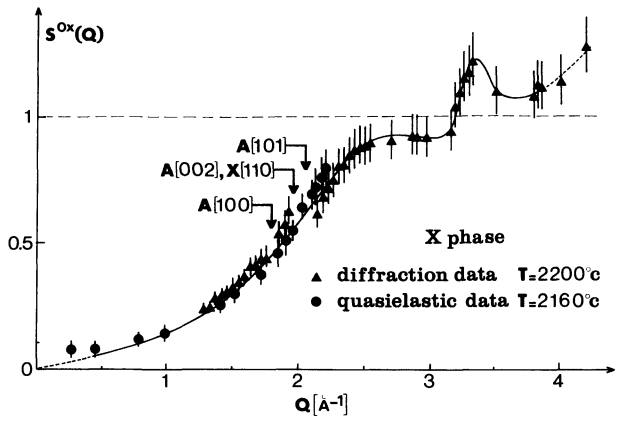

Fig. 3. — Same caption concerning the X phase of La_2O_3. One notices that the first peak in $S^{ox}(Q)$ is less pronounced in this phase than in the H phase, and its position is slightly shifted towards higher Q values.

if there exists a large number of particles at a preferred pair distance x_m. The values of x_m are respectively ~ 3 Å ($Q_m \simeq 2.6$ Å^{-1}) for the H phase and ~ 2.8 Å ($Q_m \simeq 2.75$ Å^{-1}) for the X phase. This latter distance is very close to the smallest oxygen-oxygen distance allowed by the ionic radii of O^{2-} fourfold coordinated ($r\,O^{2-(IV)} = 1.38$ Å [7]). It is also very close to the distance $a\sqrt{6}/4 = 2.76$ Å between two tetrahedral sites like 2 and 1″ as shown on figure 4. This distance between two neighbouring oxygens is the smallest one for which it is possible to give reasonable simultaneous locations for all the oxygen atoms at given time in the X-La_2O_3 structure. This will be developed in a further paper.

3. **Inelastic neutron scattering.** — Without energy analysis of scattered neutrons, there is no direct evidence of the diffusive motions of oxygens in the two high-temperature phases H and X. The IN5 multichopper time of flight spectrometer at the ILL using cold neutrons which allows measurements in the small energy transfer region, is well adapted to study this problem.

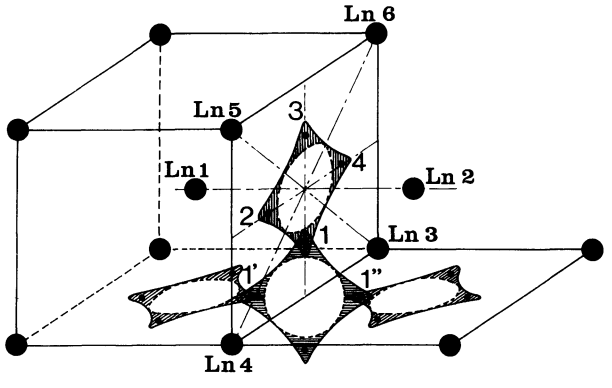

Fig. 4. — Drawing of the body centred cubic cell of the high temperature X phase of La_2O_3. The cell parameter $a = 4.51$ Å at 2 200 °C. The hatched areas on the cube faces are cross sections of the oxygen probability volume.

3.1 Experimental procedure. — The 0.25-2.20 Å^{-1} momentum transfer region has been explored with a wavelength of 4.94 Å which is a good compromise between flux and resolution. The heating device is a cold wall furnace with tungsten heater and shields, specially designed to minimize neutron scattering and absorption. It works under 1.2 atmosphere of ultra-pure helium. The sample fitted on a tungsten rod is a sintered cylinder ($L = 60$ mm, $\varnothing = 9$ mm) of pure La_2O_3 (99.9 % Pechiney-St-Gobain) with 90 % of the theoretical density. The temperature is determined by optical pyrometry at 6 500 Å in quasi blackbody conditions within an uncertainty of ± 25 °C at the highest temperature [8]. The spectra of the different phases A, H and X, shown in the figure 5, have undergone the following standard corrections : normalization with a vanadium standard, detector efficiency correction and subtraction of the empty furnace signal at an approximate temperature of 2 000 °C.

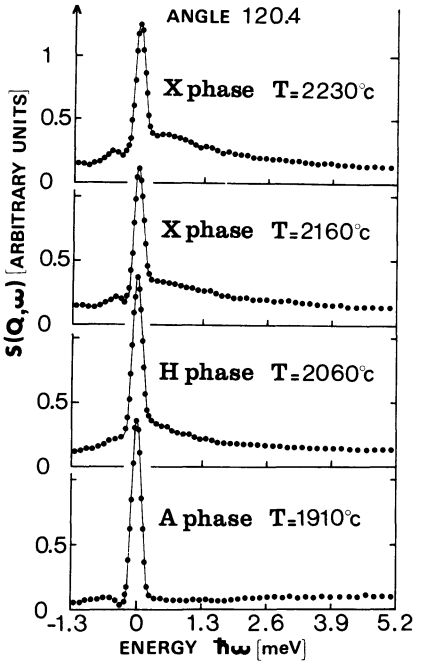

Fig. 5. — Corrected spectra for the scattering angle $2\theta = 120.4°$ for La_2O_3 in the various A, H and X high temperature phases, taken with a wavelength of 4.94 Å and a resolution of 0.22 meV FWHM. The spectra are normalized to the same number of incident neutrons. At each temperature, the spectrum of the empty furnace, at around 2 000 °C, has been subtracted.

3.2 Qualitative interpretation of the time of flight spectra. — A broad component appears in the quasielastic region (few meV) at the A → H transition (Fig. 5) which becomes slightly more intense in the X phase. At each temperature, an elastic peak remains reproducing the shape of the resolution function which is nearly triangular with a FWHM of 0.22 meV. As oxygen is a purely coherent scatterer the elastic peak in the A phase at 1 910 °C

is due only to the lanthanum incoherent cross-section and its intensity is affected by a Debye-Waller factor. The plot of log $I_{elastic}$ *versus* Q^2 (Fig. 6) gives $\langle u^2 \rangle$ the mean square displacement of lanthanum atoms. The corresponding temperature factor

$$B_{La}^{A} = 8\,\pi^2 \langle u^2 \rangle = 3.9\ \text{Å}^2$$

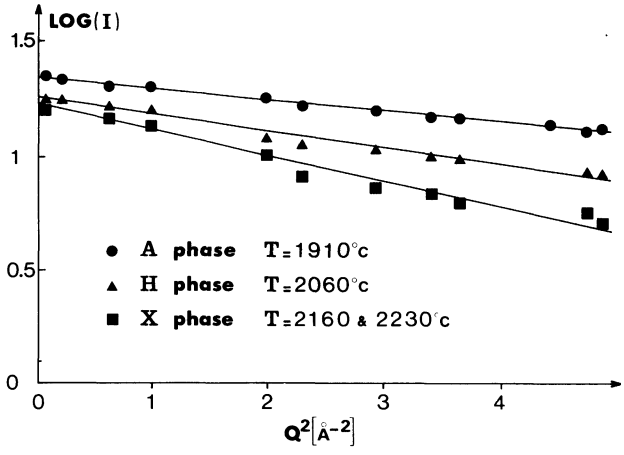

Fig. 6. — Plots of the logarithm of the intensity in arbitrary units of the elastic peak as a function of Q^2 for the various A, H, X high temperature phases of La_2O_3. The slopes of the lines give the lanthanum mean square displacement $\langle u^2 \rangle$. The decreasing intensity at $Q = 0$ with increasing temperature is due to the fact that we have subtracted the same empty furnace signal for all temperatures.

is in good agreement with our diffraction results (table I). At 2 060 °C in the H phase, using the same method, we have determined a thermal $B_{La}^{H} = 5.8$ Å^2 which is also in good agreement with our diffraction analysis. We can thus conclude that there is no significant contribution of the oxygen atoms in the elastic peak in this phase whereas on the other hand, there is evidence of their diffusive motion. This also gives some confidence in the value obtained for the thermal factor $B_{La}^{X} = 8.8$ Å^2 in the X phase which we have used in the TDS calculations. This justifies the subtraction of the A (1 910 °C) spectrum from the H and X spectra, in order to obtain the quasielastic signal in excess of the resolution width. Of course this approximate procedure is invalid in the energy region where appreciable inelastic intensity is coming from the phonon density of states of the lanthanum sublattice. In figure 7 we show the quasielastic signal for two scattering angles in the X phase at 2 160 °C. The considerable broadening reveals immediately that the oxygens are participating in fast diffusive motions.

3.3 SIMPLIFIED DYNAMICAL MODEL FOR THE X PHASE. — The total scattering function for La_2O_3 can be expressed as follows

$$S^{tot}(Q,\omega) \propto 3\,\sigma_{inc}^{(Ox)}\,S_{inc}^{(Ox)}(Q,\omega) + 2\,\sigma_{inc}^{(La)}\,S_{inc}^{(La)}(Q,\omega) + \\ + [6\,\sigma_{coh}^{(La)}\,\sigma_{coh}^{(Ox)}]^{1/2}\,[S_{coh}^{(LaOx)}(Q,\omega) + S_{coh}^{(OxLa)}(Q,\omega)] \\ + 2\,\sigma_{coh}^{(La)}\,S_{coh}^{(LaLa)}(Q,\omega) + 3\,\sigma_{coh}^{(Ox)}\,S_{coh}^{(OxOx)}(Q,\omega) \quad (8)$$

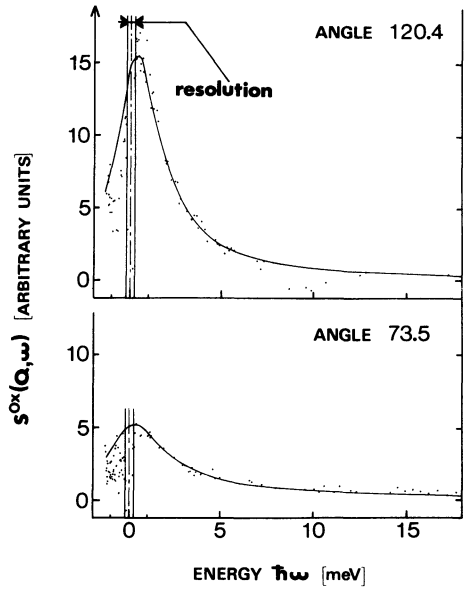

Fig. 7. — Quasielastic signal in the X-phase of La_2O_3 at 2 160 °C for two scattering angles. The points are obtained by the subtraction procedure and the full-line is the fit of our model (see text for details). The spacing between the two vertical lines is twice the FWHM of the resolution function which is nearly triangular in shape.

where σ_{inc} and σ_{coh} are the incoherent and coherent scattering cross section ; $S_{inc}(Q,\omega)$ and $S_{coh}(Q,\omega)$ are respectively the Fourier transform of the Van Hove self and pair correlation function [9]. Since $\sigma_{inc}^{(Ox)}$ is negligible, the first term disappears and the elastic peak results only from the second term. Assuming that lanthanum atoms stay around the lattice sites and that oxygen atoms are affected by a random motion uncorrelated with the periodic motion of the lanthanum atoms, one can conclude that the third and the fourth term will give rise to elastic (Bragg) and inelastic (phonon) scattering only. Thus, within the uncertainty in the inelastic region already mentioned, the quasielastic signal, in excess of the resolution width, resulting from the diffusive motion of oxygen atoms in the H and X phase can be extracted from the following subtractions : H(2 060 °C)-A (1 910 °C) and X (2 160 °C)-A (1 910 °C) (Fig. 7). The scattering in the quasielastic region due to the diffusive motion of the oxygens is thus proportional to $S_{coh}^{(OxOx)}(Q,\omega)$. The oxygen structure factor $S^{Ox}(Q)$ is experimentally deduced from the integral of this signal in the quasielastic region (typically 0-10 meV)

$$S^{Ox}(Q) = \int S_{coh}^{(OxOx)}(Q,\omega)\ d\omega\ .$$

As in the case of diffraction data a Placzek correction is applied. Since the highest accessible Q value (2.2. Å^{-1}) cannot allow the determination of $S^{Ox}(Q)$ when $Q \to \infty$, the normalization has been carried out using the diffraction data and the overlapping zone is sufficiently large to yield satisfactory good

agreement between the data from the two origins (Figs. 2 and 3).

There is no direct method for taking into account the correlated motion of pairs of oxygen atoms, but an *adhoc* approximation first applied to liquid argon [10] then to α-AgI [11] allows us to express the coherent scattering function in terms of its self part (the incoherent scattering function)

$$S_{\text{coh}}^{(\text{OxOx})}(Q, \omega) = S_{\text{inc}}^{\text{Ox}}\left[\frac{Q}{S^{\text{Ox}}(Q)^{1/2}}, \omega\right] S^{\text{Ox}}(Q) . \quad (9)$$

This approximation fulfills the moment relationships of the coherent scattering function up to the second moment [10] and gives a good phenomenological description of the line shape for the case of a simple liquid. It leads to the definition of $S_{\text{inc}}^{\text{Ox}}$ as a function of an effective momentum transfer

$$Q_{\text{eff}} = \frac{Q}{\sqrt{S^{\text{Ox}}(Q)}} .$$

In our case in the Q-domain where we have a significant quasielastic signal, i.e. $Q \simeq 0.8$ to $2.2\ \text{Å}^{-1}$, Q_{eff} shows very slight variations from $2.3\ \text{Å}^{-1}$ to $2.8\ \text{Å}^{-1}$. In order to describe the X phase quasielastic scattering and its Q dependence, different expressions for $S_{\text{inc}}^{\text{Ox}}(Q_{\text{eff}}, \omega)$ corresponding to various diffusive models have been tried. The simplest one which satisfactorily agrees with our experimental data is directly deduced from the dynamical model suggested from our previous crystallo-chemical considerations [2].

We have indeed supposed for the X phase a body centered cubic cell which can be described in the Im3m spatial group. The 2(a) positions occupied by lanthanum atoms form a rigid sublattice. Since there is no possibility of locating the oxygen atoms from refinements of the crystallographic data, simple geometrical considerations based upon ionic radii [7] in the hard sphere approximation can give some information. This leads us to exclude the 6(b) 0, 1/2, 1/2 positions and to locate reasonably the oxygen atoms either in the 12(d) 1/4, 0, 1/2 positions (occupation number 1/4) or in the 24(g) x, 0, 1/2 ; 1/2-x, 0, 1/2 (occupation number 1/8) with $x = 0.315$. With a cell parameter $a = 4.51$ Å, the distance between two adjacent 24(g) sites (x, 0, 1/2 and 1/2-x, 0, 1/2) inside the same distorted lanthanum tetrahedron is 0.59 Å. This distance can be readily accounted for in term of a mean square displacement by an anisotropic and anharmonic Debye-Waller temperature factor applied to the corresponding 1/4, 0, 1/2 12(d) site. In the very similar problem posed by the location of the silver ions in α-AgI, recent work [12, 13, 14] has demonstrated the validity of this assertion. Figure 4 represents the X body centered cubic cell which contains two lanthanide atoms and three oxygen atoms, i.e. one in each face located in one of the four tetrahedral possible sites. An oxygen in the position 1 (center of the Ln1Ln2Ln3Ln4 tetrahedron) has four possible paths, equivalent on a pure crystallographic point of view, to reach a neighbouring tetrahedral site. Nevertheless we can distinguish the $1 \rightarrow 2$ and $1 \rightarrow 4$ paths which suggest that the oxygens are confined in the same face from the $1 \rightarrow 1'$ and $1 \rightarrow 1''$ paths which bring the oxygen in another face. Thus the first two paths can be considered as elements of a local motion of the oxygen atom around the Ln1Ln2 axis over the positions 1, 2, 3, 4 whilst the last two paths can be considered as elements of a long range translational diffusive motion.

With the hypothesis of the independence of these two types of motions, $S_{\text{inc}}^{\text{Ox}}(Q_{\text{eff}}, \omega)$ which defines the dynamics of a single particle, can be written as the following convolution product [15]

$$S_{\text{inc}}^{\text{Ox}}(Q_{\text{eff}}, \omega) = S_{\text{inc}}^{\text{L}}(Q_{\text{eff}}, \omega) \otimes S_{\text{inc}}^{\text{T}}(Q_{\text{eff}}, \omega) \quad (10)$$

$S_{\text{inc}}^{\text{L}}(Q_{\text{eff}}, \omega)$ is related to the local motion which can be approximated in this case by a succession of jumps between 4 sites equally spaced on a circle of radius $\rho = a/4 = 1.13$ Å. This can be expressed [15] as follows

$$S_{\text{inc}}^{\text{L}}(Q_{\text{eff}}, \omega) = A_0(Q_{\text{eff}})\, \delta(\omega) + \frac{1}{\pi} \sum_{l=1}^{l=3} A_l(Q_{\text{eff}}) \frac{\tau_l}{1 + \omega^2 \tau_l^2} \quad (11)$$

with

$$A_l(Q_{\text{eff}}) = \frac{1}{4} \sum_{j=1}^{j=4} \times \frac{\sin\left(2\, Q_{\text{eff}}\, \rho \sin \frac{\pi j}{4}\right)}{2\, Q_{\text{eff}}\, \rho \sin \frac{\pi j}{4}} \cos\left(2\, l \frac{\pi j}{4}\right).$$

The correlation times τ_l are given by $\tau_l = \dfrac{\tau \sin^2 \pi/4}{\sin^2 \pi l/4}$ where τ is the mean jump time between adjacent sites.

$S_{\text{inc}}^{\text{T}}(Q_{\text{eff}}, \omega)$ is related to the long range translational diffusive motion. The Chudley and Elliott model [16] if the jump time $\tau_1 \ll \tau_0$ the residence time or the Gissler and Stump model [17] if τ_1 is of the order of τ_0, are frequently used in similar cases to express the translational scattering law. Nevertheless, the simplest solution consists in taking a translational self diffusion model which is described by the single Lorentzian curve

$$S_{\text{inc}}^{\text{T}}(Q_{\text{eff}}, \omega) = \frac{1}{\pi} \frac{D_{\text{T}}\, Q_{\text{eff}}^2}{(D_{\text{T}}\, Q_{\text{eff}}^2)^2 + \omega^2} \quad (12)$$

where D_{T} is the translational diffusion coefficient. It should be noted that this approximation is valid only because of the very slight variations of Q_{eff}

in the considered Q domain. The jump distance $l = a/\sqrt{8} = 1.59$ Å is related to D_T and to the jump time τ_T by the Einstein relation $l^2 = 6\, D_T\, \tau_T$.

Since in the X phase, in contradistinction with the H phase, there is no reason to prefer one of those two motions because of the symmetry of the structure, we suppose $\tau = \tau_T$, which corresponds to the Chudley-Elliott model [16]. This leads to the determination of only one parameter D_T, in the theoretical expression of the total scattering function. We have thus compared the eq. (10) with the experimental quasielastic spectra using an overall normalization factor. For the X phase at 2 160 °C, the best adjustment is obtained for $D_T = 3 \times 10^{-5}$ cm²/s with an uncertainty of about 15 %. This corresponds to a mean jump time $\tau = 1.4 \times 10^{-12}$ s. We have verified that a purely local motion, as given by eq. (11) does not fit the data at all. On the other hand, as expected, the simple diffusion model, eq. (12), gives a satisfactory fit to the data but with a diffusion coefficient about 50 % higher. Nevertheless, we prefer to distinguish between the two types of motions, since the model with $\tau \neq \tau_T$ will certainly be necessary to describe the motion of oxygen atoms in the H phase. Figure 7 gives example of the agreement obtained by using eq. (10) for two scattering angles. The small discrepancy at ω around 9 meV is interpreted as an overcorrection in the difference procedure we have used, since in this region there is an appreciable inelastic intensity in the A phase at 1 910 °C. Similarly the dip in the experimental spectra at ω around − 1 meV is certainly an overcorrection from the empty furnace signal, since that one presents a peak in this region. It is to be noticed that the signal is asymmetric and not centred at $\omega = 0$, as it is the case for a purely incoherent scatterer performing some kind of diffusive motion. This is a consequence of the coherence correction (eq. (9)) together with the fact that the spectra are not taken at constant Q but at constant scattering angle. The rather good agreement obtained with only *one adjustable parameter* offers strong support for the simple dynamical model we have used.

According to the modified Nernst-Einstein relation, one can calculate the conductivity [18]

$$\sigma = \frac{1}{f} \cdot \frac{D_T\, N e^2}{k_B\, T}$$

where N is the number of charge carriers per cm³, e the charge and f a correlation factor which is unknown in our case. This factor which takes into account correlation effects in the diffusion mechanism is usually of the order 0.5-1. In the framework of our simplified dynamical model all the oxygen ions are participating in the diffusion process, so $N = 3.3 \times 10^{22}$. In the absence of correlations, which is an improbable case, $f = 1$ and one calculates $\sigma \sim 3\ (\Omega.\mathrm{cm})^{-1}$. If $f = 0.5$ then it leads to $\sigma \sim 6\ (\Omega.\mathrm{cm})^{-1}$. In any case these are very high values for ionic conductivity.

4. **Conclusion.** — The existence of fast long range motions of oxygen ions in the X phase of the lanthanum sesquioxide has been demonstrated. The oxygens which occupy one fourth of the 12(d) 1/4, 0, 1/2 positions, diffuse through the faces of the lanthanum tetrahedra to an adjacent and empty tetrahedral site. This confirms our previous crystallochemical considerations [2] which suggested the possibility of such a diffusion path through the maximum density 110 planes of the X body centred cubic cell. The concordance of the results obtained by means of neutron diffraction and neutron quasielastic scattering clearly shows their complementarity and their ability to give structural and dynamical information on powdered samples in a temperature range where no other direct technique is at the present time available. This work has to be considered only as a first, but important step in the understanding of the high temperature polymorphism of the rare earth sesquioxides. As we have also given evidence of fast oxygen diffusive motions in the H phase, the next step will consist in the development of a diffusion model which satisfactorily takes into account the quasielastic data ; the problem is rather more complicated than for the X phase, because of the existence of two inequivalent kinds of oxygen atoms.

Acknowledgments. — We would like to thank Dr. F. Volino and Dr. P. Chieux for numerous discussions, Professor J. Joffrin for critically reading the manuscript and MM. C. Rouchon, Y. Blanc and S. Jenkins for their technical assistance.

References

[1] TRAVERSE, J. P., Thèse, Grenoble (1971).
[2] ALDEBERT, P., TRAVERSE, J. P., *Mat. Res. Bull.* **14** (1979) 303.
[3] HOSHINO, S., *J. Phys. Soc. Japan* **12** (1957) 315.
[4] FUESS, H., FUNKE, K. and KALUS, J., *Phys. Status Solidi* (a) **32** (1975) 101.
[5] BERTAGNOLLI, H., CHIEUX, P. and ZEIDLER, M. D., *Mol. Phys.* **32** (1976) 759.
[6] GUINIER, A., *Théorie et Technique de la Radiocristallographie* (Editions Dunod, Paris) 1956, p. 451.
[7] SHANNON, R. D., *Acta Crystallogr.* A **32** (1976) 751.
[8] ALDEBERT, P., BADIE, J. M., TRAVERSE, J. P., BUEVOZ, J. L. et ROULT, G., *Rev. Int. Hautes Temp. Refract.* **12** (1975) 307.
[9] EGELSTAFF, P. A., (Ed), *Thermal Neutron Scattering* (Academic Press) 1965.

[10] SKÖLD, K., *Phys. Rev. Lett.* **19** (1967) 1023.
[11] ECKOLD, G., FUNKE, K., KALUS, J. and LECHNER, R. E., *J. Phys. Chem. Solids* **37** (1976) 1097.
[12] HOSHINO, S., SAKUMA, T. and FUJII, Y., *Solid State Commun.* **22** (1977) 763.
[13] CAVA, R. J., REIDINGER, F. and WUENSCH, B. J., *Solid State Commun.* **24** (1977) 411.
[14] COOPER, M. J. and SAKATA, M., AERE Report (1978).
[15] DIANOUX, A. J., VOLINO, F. and HERVET, H., *Mol. Phys.* **30** (1975) 1181.
VOLINO, F. and DIANOUX, A. J., *Proc. Euchem. Conf.* « *Organic Liquids* » (John Wiley & Sons Ltd) 1978, p. 29.
[16] CHUDLEY, C. T. and ELLIOTT, R. J., *Proc. Phys. Soc.* **77** (1961) 353.
[17] GISSLER, W. and STUMP, N., *Physica* **65** (1973) 109.
[18] HAVEN, Y., *Solid Electrolytes* (Academic Press) 1978, p. 59.